Journal of Alloys and Compounds 505 (2010) L31–L34

Contents lists available at ScienceDirect

Journal of Alloys and Compounds

journal homepage: www.elsevier.com/locate/jallcom

Letter

Consolidation and mechanical properties of nanostructured $MoSi_2$ from mechanically reacted powder by high-frequency induction-heated sintering

In-Yong Ko[a], Jeong-Hwan Park[a,b], Jin-Kook Yoon[c], Jung-Mann Doh[c], In-Jin Shon[a,b,*]

[a] Division of Advanced Materials Engineering, the Research Center of Advanced Materials Development, Chonbuk National University, 664-14 Deokjin-dong 1-ga, Deokjin-gu, Jeonju, Jeonbuk 561-756, Republic of Korea
[b] Department of Hydrogen and Fuel Cells Engineering, Specialized Graduate School, Chonbuk National University, 664-14 Deokjin-dong 1-ga, Deokjin-gu, Jeonju, Jeonbuk 561-756, Republic of Korea
[c] Advanced Functional Materials Research Center, Korea Institute of Science and Technology, PO Box 131, Cheongryang, Seoul 130-650, Republic of Korea

ARTICLE INFO

Article history:
Received 2 July 2009
Accepted 12 June 2010
Available online 30 June 2010

Keywords:
Nanostructured material
Powder metallurgy
Sintering
Mechanical properties

ABSTRACT

Dense nanostructured $MoSi_2$ was sintered from a mechanically synthesized powder of $MoSi_2$ within 1 min using a high-frequency induction heating method. $MoSi_2$ with a relative density of up to 97% was produced by the simultaneous application of a 60 MPa pressure and an induced current. The average grain size of the $MoSi_2$ sample was approximately 100 nm. The hardness and fracture toughness of the sample was 1203 kg/mm^2 and 4.2 MPa m$^{1/2}$, respectively.

1. Introduction

$MoSi_2$ has been investigated as a potential material for high-temperature structural and electronic applications. $MoSi_2$ has a desirable combination of a high melting temperature (2020 °C), high modulus (440 GPa), good oxidation resistance in air, a relatively low density (6.24 g/cm^3) [1], and the ability to undergo plastic deformation above 1200 °C [2]. Combined with the good thermal and electric conductivity, these properties led to the use of $MoSi_2$ as a heating element material in high-temperature furnaces operating in air up to approximately 1700 °C [3,4]. However, as in the case of many such compounds, there is considerable concern regarding its low fracture toughness below the ductile–brittle transition temperature [5,6]. The fabrication of nanostructured materials has been found to be effective in improving the mechanical properties of these materials. Nanocrystalline materials have attracted considerable attention as advanced engineering materials with improved physical and mechanical properties [7,8]. More attention has been paid to the application of nanomaterials on account of their high strength, high hardness, excellent ductility and toughness [9,10]. Recently, nanocrystalline powders have been developed by thermochemical and thermomechanical processes, such as the spray conversion process (SCP), co-precipitation and high-energy milling [6,11,12]. However, the grain size in sintered materials is much larger than that of the pre-sintered powders due to the rapid grain growth that occurs during conventional sintering. Therefore, although the initial particle size is <100 nm, the grain size increases rapidly up to 500 nm or larger during conventional sintering [13]. Therefore, controlling grain growth during sintering is essential to the commercial success of nanostructured materials. In this regard, the high-frequency induction-heated sintering method, which can produce dense materials within 2 min, has been shown to be effective in achieving this goal [14,15].

This paper reports an investigation of the fabrication of $MoSi_2$ nanopowders by high-energy ball milling and the consolidation of dense nanostructured $MoSi_2$ (within 1 min) starting with the reacted nanopowder. The mechanical properties of the resulting nanostructured $MoSi_2$ were evaluated.

2. Experimental procedure

Powders of 99.999% molybdenum (−325 mesh, Alfa Products) and 99% pure silicon (−325 mesh, Aldrich Products) were used as the starting materials. Mo and Si powder mixtures were first milled in a high-energy ball mill (Pulverisette-5 planetary mill) at 250 rpm for 10 h. Tungsten carbide balls (5 mm in diameter) were used in a sealed cylindrical stainless steel vial in an argon atmosphere. A charge ratio (ratio of mass of balls to powder) of 30:1 was used.

The interaction between the Mo and 2Si during was milling is thermodynamically feasible according to the following reaction:

$$Mo + 2Si \rightarrow MoSi_2 \quad (1)$$

* Corresponding author at: Division of Advanced Materials Engineering, the Research Center of Advanced Materials Development, Chonbuk National University, Deokjin-dong 1-ga, Deokjin-gu, Jeonju, Jeonbuk 561-756, Republic of Korea. Tel.: +82 63 2381; fax: +82 63 270 2386.
E-mail address: ijshon@chonbuk.ac.kr (I.-J. Shon).

0925-8388/$ – see front matter © 2010 Elsevier B.V. All rights reserved.
doi:10.1016/j.jallcom.2010.06.119

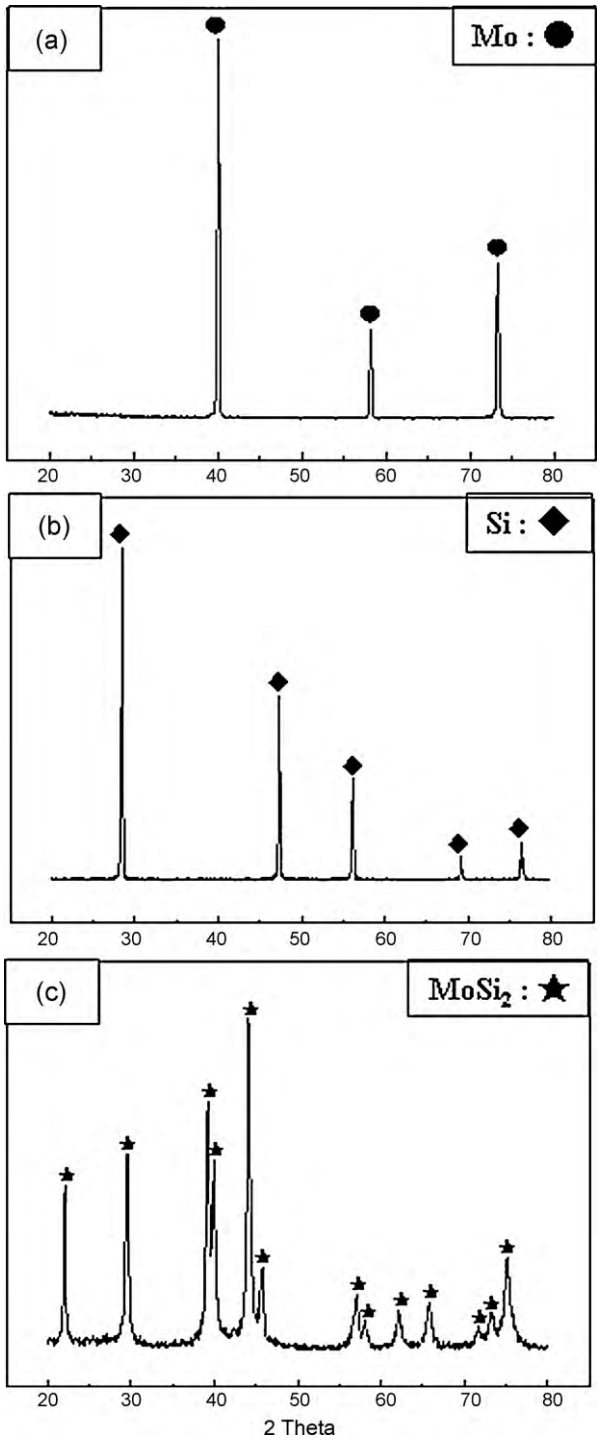

Fig. 1. XRD patterns of the raw materials: (a) Mo, (b) Si and (c) milled Mo + 2Si.

Fig. 1 shows the X-ray diffraction (XRD) patterns of the raw materials and milled powder. During milling, $MoSi_2$ was synthesized from Mo and 2Si powders, as shown in Fig. 1(c). Milling resulted in a significant decrease in the grain size of $MoSi_2$. The grain size and internal strain were calculated using Suryanarayana and Grant Norton's formula [16]:

$$B_r(B_{\text{crystalline}} + B_{\text{strain}})\cos\theta = \frac{k\lambda}{L} + \eta\sin\theta \quad (2)$$

where B_r is the full width at half-maximum (FWHM) of the diffraction peak after an instrument correction; $B_{\text{crystalline}}$ and B_{strain} are FWHM caused by the small grain size and internal stress, respectively; k is a constant (with a value of 0.9); λ is the wavelength of the X-ray radiation; L and η are the grain size and internal strain, respectively; θ is the Bragg angle. The parameters, B and B_r, follow the Cauchy's form with the relationship: $B = B_r + B_s$, where B and B_s are the FWHM of the broadened Bragg peaks and the standard Bragg peaks of the samples, respectively. The mean grain size of $MoSi_2$ determined using Suryanarayana and Grant Norton's formula was approximately 41 nm.

After milling, the powder was placed in a graphite die (outside diameter = 45 mm, inside diameter = 20 mm, and height = 40 mm) and introduced into a high-frequency induction-heated sintering system, which is shown schematically in Ref. [17]. The synthesis was performed in four major stages. The system was evacuated to 40 mTorr (stage 1), and a uniaxial pressure of 60 MPa was then applied (stage 2) followed by the activation of an induced current (≈50 kHz), which was maintained until densification was achieved, as indicated by a linear gauge measuring the shrinkage of the sample (stage 3). The temperatures were measured using a pyrometer focused on the surface of the graphite die. At the end of the process, the sample was cooled to room temperature (stage 4). The process was carried out under a vacuum of 40 mTorr.

The relative density of the sintered sample was measured using the Archimedes method. Microstructural information was obtained from the product samples that had been polished and etched for 1 min at room temperature using a solution of HF (10 vol.%), HNO_3 (20 vol.%), and H_2O (70 vol.%). The composition and microstructure of the products were determined by XRD and scanning electron microscopy (SEM) with energy dispersive X-ray analysis (EDAX). The Vickers hardness was measured by performing indentations on the sintered samples at a 1 kg load and a dwell time of 15 s.

3. Results and discussion

Fig. 2 shows the changes in shrinkage displacement and temperature of the surface of the graphite die with heating time during the sintering of $MoSi_2$. As the induced current was applied, the specimen initially showed small (thermal) expansion, and shrinkage displacement increased gradually with temperature to approximately 1100 °C, and then continuously to 1300 °C. Fig. 3 shows SEM (secondary electron) images of (a) the powder after milling, (b) the specimen heated to 1400 °C. The XRD patterns of the milled powder (Fig. 4(a)) show only the peaks pertaining to $MoSi_2$. However, when the temperature was increased to 1400 °C, XRD showed peaks for $MoSi_2$, as indicated in Fig. 4(b), along with those for a minor phase (Mo_5Si_3), as shown in Fig. 4(b). The presence of Mo_5Si_3 in the sample suggests a Si deficiency. It is believed that this observation is related to the entrapped oxygen in the pores of the interior portion of the sample during pressing or possibly to the slight oxidation of Si during heating.

The structure parameter, i.e. the average grain size of the silicide phases was estimated using Suryanarayana and Grant Norton's formula [16]. Fig. 5 shows a plot of $B_r\sin\theta$ as a function of $\cos\theta$. The intercept ($K\lambda/L$) can be used to calculate the crystallite size (L). The average grain sizes of $MoSi_2$ prepared using this method were approximately 100 nm.

The Vickers hardness of the polished sections of the $MoSi_2$ was measured using a 1 kg load and a 15 s dwell time. The calculated hardness of $MoSi_2$ was 1203 kg/mm^2. This represents an average of five measurements. Indentations with sufficiently large loads

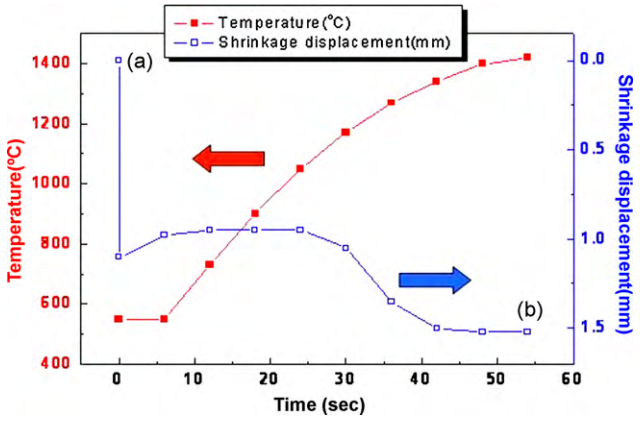

Fig. 2. Variations in temperature and shrinkage displacement with heating time during the densification of $MoSi_2$.

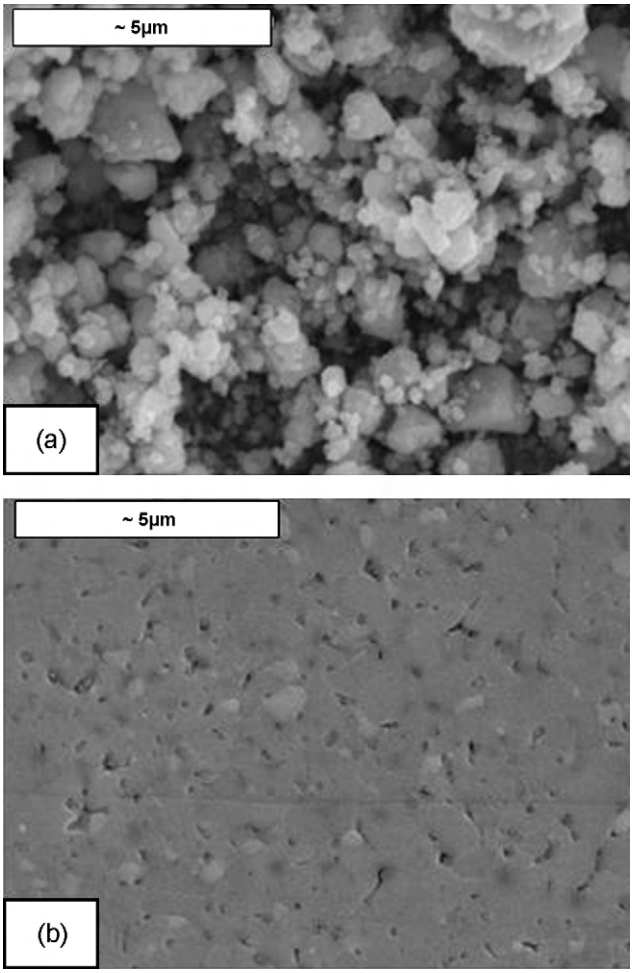

Fig. 3. Scanning electron microscope images of the Mo + 2Si system: (a) after milling and (b) after the consolidation of $MoSi_2$.

produced median cracks around the indent. From the length of these cracks, the fracture toughness can be determined using two expressions. The first expression, proposed by Anstis et al. [18] is

$$K_{IC} = 0.016\left(\frac{E}{H}\right)^{1/2}\left(\frac{P}{C}\right)^{3/2} \quad (3)$$

where E is Young's modulus, H is the indentation hardness, P is the indentation load, and C is the trace length of the crack measured

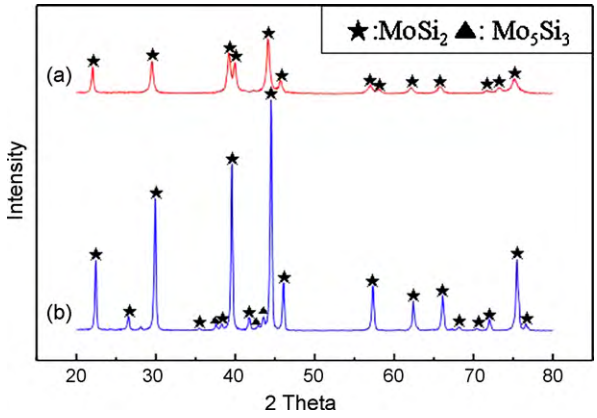

Fig. 4. XRD patterns of the Mo + 2Si system: (a) after milling and (b) after the consolidation of $MoSi_2$.

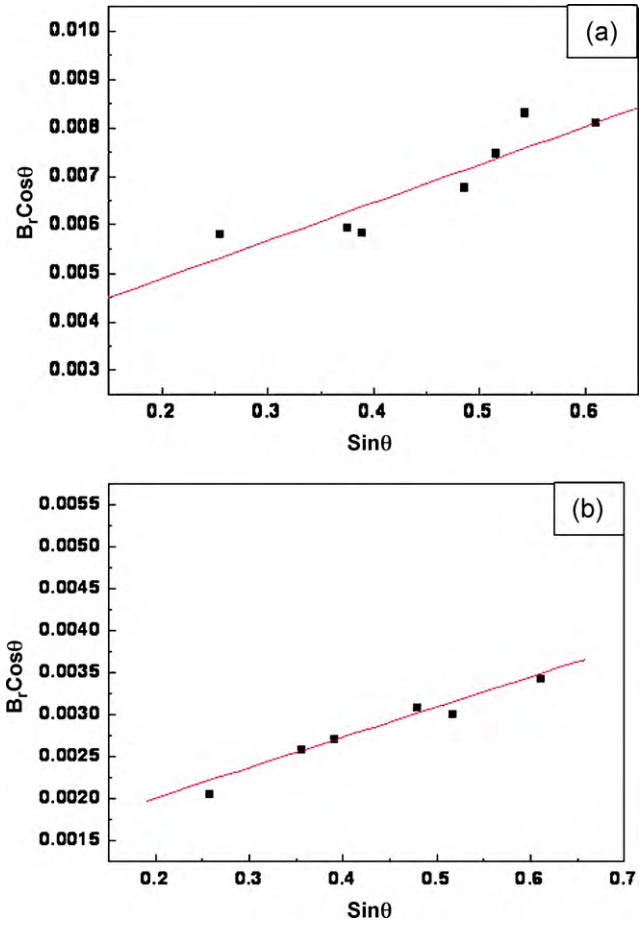

Fig. 5. Plot of $B_r \cos\theta$ versus $\sin\theta$: (a) after milling, and (b) after the consolidation of $MoSi_2$.

from the center of the indentation. The second expression proposed by Niihara et al. [19] is

$$K_{IC} = 0.023\left(\frac{c}{a}\right)^{-3/2} H_v\, a^{1/2} \quad (4)$$

where c is the trace length of the crack measured from the center of the indentation, a is the half of average length of two indent diagonals, and H_v is the hardness. The toughness values were derived from an average of five measurements. The toughness values calculated using the two methods were 4.3 ± 0.3 and 4.2 ± 0.3 MPa $m^{1/2}$, respectively. These fracture toughness and hardness values of nanostructured $MoSi_2$ were higher than those (fracture toughness; 2.58 MPa $m^{1/2}$ hardness; 8.7 MPa) of microstructured $MoSi_2$ [20] due to the refinement of the grain size.

4. Summary

$MoSi_2$ was synthesized mechanically from elemental powders of Mo and 2Si during high-energy ball milling for 10 h. Using the HFIHS method, the $MoSi_2$ was consolidated within 1 min using mechanically activated $MoSi_2$ powders. The relative density of the $MoSi_2$ was 97% of the theoretical at an applied pressure of 60 MPa. The average grain size of $MoSi_2$ prepared by the HFIHS method was approximately 100 nm. The average hardness and fracture toughness was 1203 kg/mm^2 and 4.3 MPa $m^{1/2}$, respectively. These fracture toughness and hardness of the nanostructured $MoSi_2$ were higher than those of microstructured $MoSi_2$.

Acknowledgement

This study was supported by the Korea Research Foundation Grant (KRF-2009-0065776) funded by the Korean Government (MOEHRD).

References

[1] A.K. Vasudevan, J.J. Petrovic, Mater. Sci. Eng. A 155 (1992) 259–266.
[2] R. Mitra, Y.R. Mahajan, N.E. Prasad, W.A. Chiou, C. Ganguly, Key Eng. Mater. 108–110 (1995) 11–16.
[3] J. Milne, Instant Heat, Kinetic Metals, Inc., Derby, CO, 1985.
[4] Y.S. Touloukian, R.W. Powell, C.Y. Ho, P.G. Klemens, Thermal Conductivity, IFI/Plenum, New York, 1970.
[5] G. Sauthoff, Intermetallics, VCH Publishers, New York, 1995.
[6] Y. Ohya, M.J. Hoffmann, G. Petzow, J. Mater. Sci. Lett. 12 (1993) 149–154.
[7] M.S. El-Eskandarany, J. Alloys Compd. 305 (2000) 225–238.
[8] L. Fu, L.H. Cao, Y.S. Fan, Scr. Mater. 44 (2001) 1061–1068.
[9] K. Niihara, Nikahira, Elsevier Scientific Publishing, Co., Trieste, Italy, 1990.
[10] S. Berger, R. Porat, R. Rosen, Prog. Mater. Sci. 42 (1997) 311.
[11] Z. Fang, J.W. Eason, Int. J. Refract. Met. Hard Mater. 13 (1995) 297–303.
[12] A.I.Y. Tok, l.h. Luo, F.Y.C. Boey, Mater. Sci. Eng. A 383 (2004) 229–234.
[13] M. Sommer, W.D. Schubert, E. Zobetz, P. Warbichler, Int. J. Refract. Met. Hard Mater. 20 (2002) 41–50.
[14] C.D. Park, H.C. Kim, I.J. Shon, Z.A. Munir, J. Am. Ceram. Soc. 85 (2002) 2670–2677.
[15] H.C. Kim, I.J. Shon, J.K. Yoon, J.M. Doh, Met. Mater. Int. 12 (2006) 141–146.
[16] C. Suryanarayana, M. Grant Norton, X-ray Diffraction: A Practical Approach, Plenum Press, New York, 1998.
[17] H.C. Kim, I.J. Shon, I.K. Jeong, I.Y. Ko, J.K. Yoon, J.M. Doh, Met. Mater. Int. 13 (2007) 39–45.
[18] G.R. Anstis, P. Chantikul, B.R. Lawn, D.B. Marshall, J. Am. Ceram. Soc. 64 (1981) 533–538.
[19] K. Niihara, R. Morena, D.P.H. Hasselman, J. Mater. Sci. Lett. 1 (1982) 12.
[20] K. Robert, Wade, J. Am. Ceram. Soc. 75 (1992) 1682–1684.